

Design of Lead-Lag Compensators for Robust Control

Roberto Zanasi and Stefania Cuoghi

Abstract—In this paper three different methods for the synthesis of lead-lag compensators that meet design specifications on the phase margin and the gain crossover frequency are presented. These numerical and graphical methods are based on the choice of a degree of freedom of the regulators. These procedures aim to satisfy an additional specification for robust control: the gain margin, the complementary modulus margin or a specification on the settling time of the controlled system.

I. INTRODUCTION

In recent years the literature shows a renewed interest in the design of classical lead and lag types controllers [1]–[4]. In some cases second order lead-lag controllers, compared with the most widely used PID regulators, lead to a better tradeoff between the static accuracy, system stability and insensibility to disturbance in frequency domain [5]. This paper focuses on the design of lead-lag compensators characterized by real or complex zeros and poles and by a unitary static gain. They are used to control linear time invariant (LTI) plants which may include the gain or the integration terms to meet the steady-state accuracy specifications. The form of the considered compensators has three degrees of freedom that can be used to satisfy three dynamical specifications. Two of them are designed to meet the phase margin and the gain crossover frequency. These frequency specifications are known to be related to the peak overshoot, the rise time and the bandwidth of the closed-loop system. Properties on variations of the third freedom degree of the lead-lag compensators and the controlled system are given. Some methods to meet the settling time of the controlled system step response, the gain margin and the complementary modulus margin are proposed and compared. They are based on the root locus method and on the so called *inversion formulae* method, that is an extension of the modified Ziegler-Nichols method, see [6] pp. 140 – 142. This technique has been applied so far to the continuous and discrete lead and lag regulators [4] and to the continuous lead-lag compensators [7] to satisfy gain margin, phase margin and crossover frequency specifications. In this paper the *inversion formulae* method is extended to satisfy the complementary modulus margin related to the infinity-norm of complementary sensitivity function. Simulation results show the effectiveness of the proposed methods. The paper is organized as follows: in Section II, the properties of lead-lag compensators that

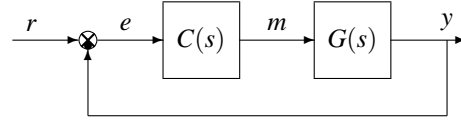


Fig. 1. Unity feedback control structure.

meet the phase margin and the gain crossover frequency are presented. In Section III three methods to meet settling time, gain margin and complementary modulus margin are proposed. In Section IV numerical examples are given. The comparison between the methods and the conclusions end the paper.

II. PROPERTIES OF LEAD-LAG COMPENSATORS

Consider the block diagram of the system shown in Fig. 1 where $G(s)$ denotes the transfer function of the LTI plant to be controlled and $C(s)$ denotes the lead-lag compensator to be design. Function $G(s)$ is supposed to include the gain and the integration terms required to meet the steady-state accuracy specifications. The considered lead-lag compensator including real or complex zeros and poles has the following form:

$$C(s) = \frac{s^2 + 2\gamma\delta\omega_n s + \omega_n^2}{s^2 + 2\delta\omega_n s + \omega_n^2}, \quad (1)$$

where parameters γ , δ and ω_n are real and positive. The synthesis of these parameters does not change the static behavior of the controlled system, since the static gain of $C(s)$ is unity. The frequency response $C(j\omega)$ can be written as

$$C(j\omega) = \frac{1 + jX(\omega)}{1 + jY(\omega)}, \quad (2)$$

where

$$X(\omega) = \frac{2\gamma\delta\omega\omega_n}{\omega_n^2 - \omega^2}, \quad Y(\omega) = \frac{2\delta\omega\omega_n}{\omega_n^2 - \omega^2}. \quad (3)$$

Since γ , δ and ω_n are real and positive, functions $X(\omega)$ and $Y(\omega)$ are positive when $\omega < \omega_n$ and negative when $\omega > \omega_n$.

The Nyquist and the Bode diagrams of $C(j\omega)$ for $\omega_n = 1$ and for different values of the parameters δ and γ are shown in Fig. 2 and 3. In particular, the Nyquist diagram of $C(j\omega)$ is a circle which intersects the real axis at point (1,0) for $\omega \in \{0, \infty\}$ and at point $(\gamma, 0)$ for $\omega = \omega_n$, see [8]. From this property it follows that γ is the maximum (or minimum) amplitude of the compensator $C(s)$ when $\gamma > 1$ (or $\gamma < 1$). Parameter γ can be expressed as follows

$$\gamma = C(j\omega_n) = \lim_{\omega \rightarrow \omega_n} \frac{X(\omega)}{Y(\omega)}. \quad (4)$$

R. Zanasi and S. Cuoghi are with the Faculty of Engineering, DII-Information Engineering Department, University of Modena and Reggio Emilia, Via Vignolese 905, 41100, Modena, Italy, e-mails: roberto.zanasi@unimore.it and stefania.cuoghi@unimore.it.

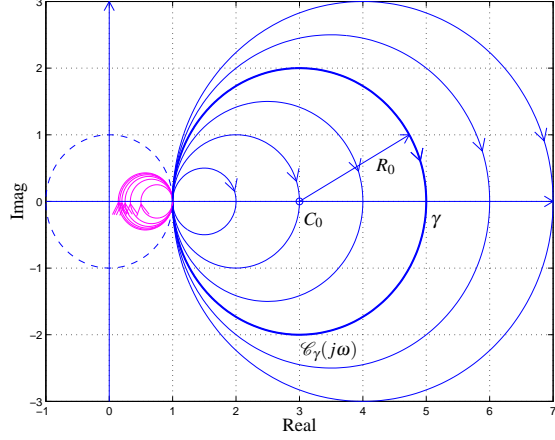


Fig. 2. Nyquist diagrams of function $C(j\omega)$ when $\omega_n = 1$, ($\delta = 1.5$, $\gamma = [2 : 1 : 7]$, blue lines) and ($\gamma\delta = 1.5$, $\gamma = 1./[2 : 1 : 7]$, magenta lines). The thick blue line is for $\delta = 1.5$ and $\gamma = 5$.

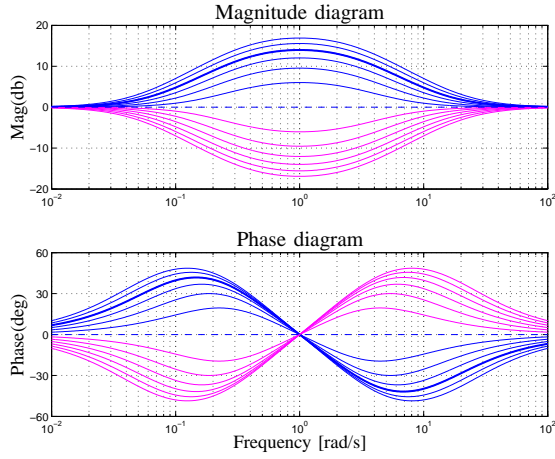


Fig. 3. Bode diagrams of function $C(j\omega)$ when $\omega_n = 1$, ($\delta = 1.5$, $\gamma = [2 : 1 : 7]$, blue lines) and ($\gamma\delta = 1.5$, $\gamma = 1./[2 : 1 : 7]$, magenta lines). The thick blue line is for $\delta = 1.5$ and $\gamma = 5$.

In Fig. 2, the circle $\mathcal{C}_\gamma(j\omega)$ denotes the set of all the frequency responses $C(j\omega)$ having the same parameter γ .

Design Problem. Find the parameters γ , δ and ω_n of $C(s)$ in order to exactly satisfy the phase margin ϕ_m specification at a given gain crossover frequency ω_0 .

The solution of the Design Problem can be exactly obtained using the modified Ziegler-Nichols method. Chosen an arbitrary point $A = M_A e^{j\varphi_A}$ on the Nyquist curve of plant $G(s)$ at the frequency ω_0 , this method tries to find the controller that moves this point to a suitable point $B = M_B e^{j\varphi_B}$ where the loop gain frequency response satisfies the given margin specification. Using the same notations introduced in [8], let $C(j\omega_0) = M_0 e^{j\varphi_0}$ denote the value of the frequency response $C(j\omega) = M(\omega) e^{j\varphi(\omega)}$ at frequency ω_0 , where $M_0 = M(\omega_0)$ and $\varphi_0 = \varphi(\omega_0)$. Referring to Fig. 4, we say that *point A is controllable to point B* (or equivalently that *point A can be moved to point B*) if a value $C(j\omega_0)$ exists

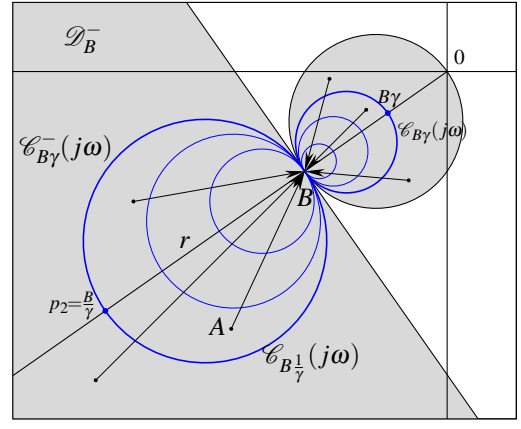


Fig. 4. Controllable domain \mathcal{D}_B^- on the Nyquist plane.

such that $B = C(j\omega_0) \cdot A$, that is if and only if the following conditions hold:

$$M_B = M_A M_0, \quad \varphi_B = \varphi_A + \varphi_0. \quad (5)$$

Definition 1: (\mathcal{D}_B^-) Given a point $B \in \mathbb{C}$, the “controllable domain \mathcal{D}_B^- of lead-lag compensator $C(s)$ to point B ” is defined as follows

$$\mathcal{D}_B^- = \left\{ A \in \mathbb{C} \mid \exists \gamma, \delta, \omega_n > 0, \exists \omega \geq 0 : C(j\omega) \cdot A = B \right\}.$$

The shape of region \mathcal{D}_B^- is shown in gray in Fig. 4. \triangle

Definition 2: (Inversion Formulae) Given two points $A = M_A e^{j\varphi_A}$ and $B = M_B e^{j\varphi_B}$ of the complex plane \mathbb{C} , the lead-lag inversion formulae $X(A, B)$ and $Y(A, B)$ are defined as follows

$$X(A, B) = \frac{M - \cos \varphi}{\sin \varphi}, \quad (6)$$

$$Y(A, B) = \frac{\cos \varphi - \frac{1}{M}}{\sin \varphi},$$

where $M = \frac{M_B}{M_A}$ and $\varphi = \varphi_B - \varphi_A$. \triangle

These equations are the same inversion formulae introduced in [9] and used in [7] and [4].

Property 1: (From A to B) Given a point $B \in \mathbb{C}$ and chosen a point A of the frequency response $G(j\omega)$ at frequency ω_A belonging to the controllable domain \mathcal{D}_B^- , i.e., $A = G(j\omega_A) \in \mathcal{D}_B^-$, the set $\mathcal{C}(s, \omega_n)$ of all the lead-lag compensators $C(s)$ that move point A to point B is obtained from (1) using the parameters

$$\gamma = \frac{X(A, B)}{Y(A, B)} > 0, \quad \delta = Y(A, B) \frac{\omega_n^2 - \omega_A^2}{2\omega_n \omega_A} > 0 \quad (7)$$

for all $\omega_n > 0$ such that $\delta > 0$ and with parameters $X(A, B)$ and $Y(A, B)$ obtained using the inversion formulae (6).

The substitution of relations (7) in (1) yields to the following expression $C(s, \omega_n)$ of all the compensators (1) that move the

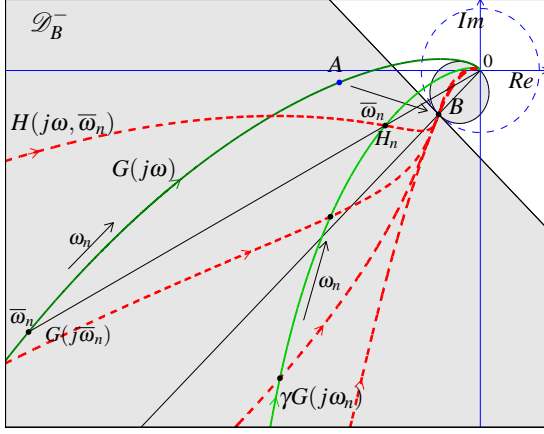


Fig. 5. The Nyquist plots of the set of $H(j\omega, \omega_n)$ passing on B and graphical interpretation of $\gamma G(j\omega)$.

point A to the point B

$$C(s, \omega_n) = \frac{s^2 + \frac{X(A,B)}{\omega_A}(\omega_n^2 - \omega_A^2)s + \omega_n^2}{s^2 + \frac{Y(A,B)}{\omega_A}(\omega_n^2 - \omega_A^2)s + \omega_n^2}. \quad (8)$$

Design specifications on the phase margin ϕ_m at a given crossover frequency ω_A are satisfied if point A is chosen such that $A = G(j\omega_A)$ and point B is chosen on the unitary circle: $B = e^{j(\pi + \phi_m)}$. In this way all the loop gain frequency responses $H(j\omega, \omega_n) = G(j\omega)C(j\omega, \omega_n)$, for $\omega_n \in (0, \omega_A)$, pass through the required point B , see Fig. 5. However the choice of the parameter ω_n influences heavily the close-loop performances and stability [10]. Compensators $C(s, \omega_n)$ satisfy the following Properties 2 and 3.

Property 2: All the frequency responses $C(j\omega, \omega_n)$, for $\omega_n \in (0, \omega_A)$, have the same parameter γ and the same shape on the Nyquist diagram: a circle with center $C_0 = \frac{\gamma+1}{2}$ and radius $R_0 = \frac{|\gamma-1|}{2}$ (see Fig. 6). The value of parameter ω_n modifies the distribution of the frequencies ω on the Nyquist diagram, except for frequency ω_A corresponding to the point $C_A = C(j\omega_A, \omega_n)$, which is constant and does not depend on ω_n :

$$C_A = C(j\omega_A, \omega_n) = \frac{1 + jX(A,B)}{1 + jY(A,B)} = C(j\omega_A). \quad (9)$$

Similarly, the Bode diagrams of $C(j\omega, \omega_n)$ when $\omega_n \in (0, \omega_A)$ are shown in Fig. 7: the blue highlighted points $C_n(\omega_n)$ denote the magnitudes and the phases of $C(j\omega, \omega_n)$ at frequency ω_n . Only point C_A does not change its magnitude and its phase when ω_n varies.

Property 3: Given the loop gain frequency response $H(j\omega, \bar{\omega}_n) = G(j\omega)C(j\omega, \bar{\omega}_n)$ for a particular value $\bar{\omega}_n \in (0, \omega_A)$, the point $H_n = H(j\omega_n, \bar{\omega}_n)|_{\omega=\omega_n}$ is $H_n = \gamma G(j\bar{\omega}_n)$. Point H_n can be graphically determined on the Nyquist plane as the point $\gamma G(j\bar{\omega}_n)$ where function $H(j\omega, \bar{\omega}_n)$ intersects the straight line passing through points $G(j\bar{\omega}_n)$ and 0. So, for $\omega_n \in (0, \omega_A)$, the function $\gamma G(j\omega_n)$ is the locus of all the

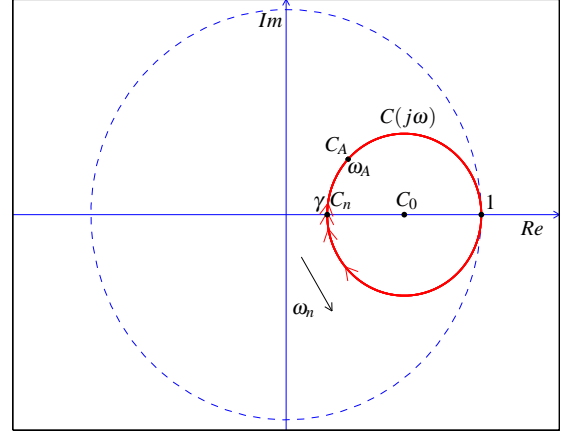


Fig. 6. The Nyquist diagrams of $C(j\omega, \omega_n)$ on variations of ω_n .

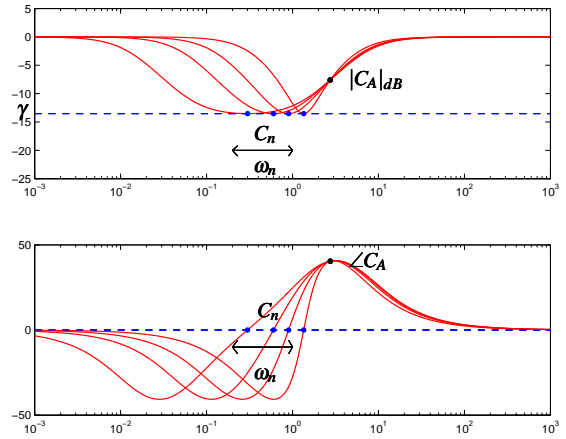


Fig. 7. The Bode diagrams of $C(j\omega, \omega_n)$ on variations of ω_n .

points of the loop gain frequency responses $H(j\omega, \omega_n) = C(j\omega, \omega_n)G(j\omega)$ at frequency $\omega = \omega_n$, see Fig. 5.

The proof follows directly from Prop. 2 and from the fact that, for every $\omega_n \in (0, \omega_A)$, it is

$$H(j\omega_n, \omega_n) = C(j\omega_n, \omega_n)G(j\omega_n) = \gamma G(j\omega_n). \quad (10)$$

III. HOW TO CHOOSE THE DEGREE OF FREEDOM ω_n

Given the compensators (8), which satisfy design specifications on phase margin and gain crossover frequency, let us consider different methods to choose the value of parameter ω_n .

A. Constraint on the settling time t_s

Design Problem A: (ϕ_m, ω_p, t_s). Given the control scheme of Fig. 1, the transfer function $G(s) = \frac{N(s)}{D(s)}$ and design specifications on phase margin ϕ_m and gain crossover frequency ω_p , design the lead-lag compensator $C(s)$ such that the loop gain frequency response $C(j\omega)G(j\omega)$ passes through point $B_p = e^{j(\pi + \phi_m)}$ for $\omega = \omega_p$ and the step response of the closed-loop system has its minimum settling time t_s .

Solution A: From Prop. 1, design specifications on the phase margin ϕ_m and gain crossover frequency ω_p are

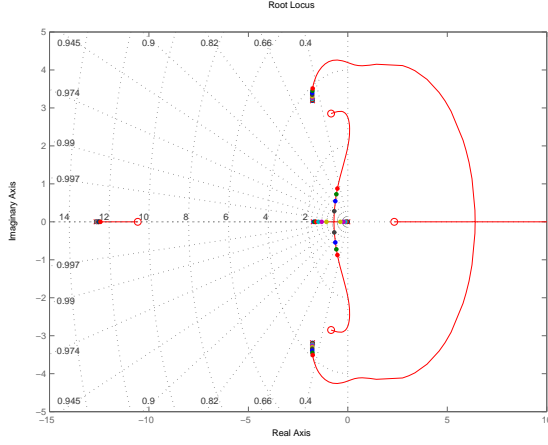


Fig. 8. Root locus of $1 + \omega_n^2 \bar{G}(s)$ for $\omega_n^2 \in (0, \infty)$.

exactly satisfied by the the lead-lag compensators $C(s, \omega_n)$ in (8), with $\omega_A = \omega_p$, $A = G(j\omega_p)$ and $B_p = e^{j(\pi + \phi_m)}$. The degree of freedom ω_n can be used to satisfy the constraint on the settling time. In this case the classical root locus and the contour locus methods can be used. It can be easily shown that the set of the closed-loop characteristic equations

$$1 + G(s)C(s, \omega_n) = 0 \quad (11)$$

can be expressed as follows:

$$1 + \omega_n^2 \bar{G}(s) = 0, \quad (12)$$

where

$$\bar{G}(s) = \frac{D(s)(\omega_p + Y(A, B)s) + N(s)(\omega_p + X(A, B)s)}{\omega_p s(D(s)(s - Y(A, B)\omega_p) + N(s)(s - X(A, B)\omega_p))}.$$

The settling time t_s can be minimized choosing parameter ω_n such to maximize the distance of the poles from the imaginary axis on the root locus of $\bar{G}(s)$ when $\omega_n^2 \in (0, \omega_A^2)$, see Fig. 8.

B. Constraint on the gain margin G_m

Design Problem B: (ϕ_m, ω_p, G_m) . Given the control scheme of Fig. 1, the transfer function $G(s)$ and design specifications on the phase margin ϕ_m , gain margin G_m and gain crossover frequency ω_p , design a lead-lag compensator $C(s)$ such that the loop gain frequency response $C(j\omega)G(j\omega)$ passes through point $B_p = e^{j(\pi + \phi_m)}$ for $\omega = \omega_p$ and passes through point $B_g = -1/G_m$.

Solution B: The solution can be obtained graphically and numerically as follows, see [8].

Step 1. Draw the controllable domain $\mathcal{D}_{B_p}^-$ of point $B_p = e^{j(\pi + \phi_m)}$ as shown in Fig. 9 and check whether the point $A_p = G(j\omega_p)$ belongs to $\mathcal{D}_{B_p}^-$. If not the Design Problem has no acceptable solutions.

Step 2. Determine the parameters $X_p = X(A_p, B_p)$, $Y_p = Y(A_p, B_p)$ using the inversion formulas (6).

Step 3. Draw the circle $\mathcal{C}_{B_g\gamma}^-(j\omega)$ having its diameter on the segment defined by points B_g and $\frac{B_g}{\gamma}$, where $B_g =$

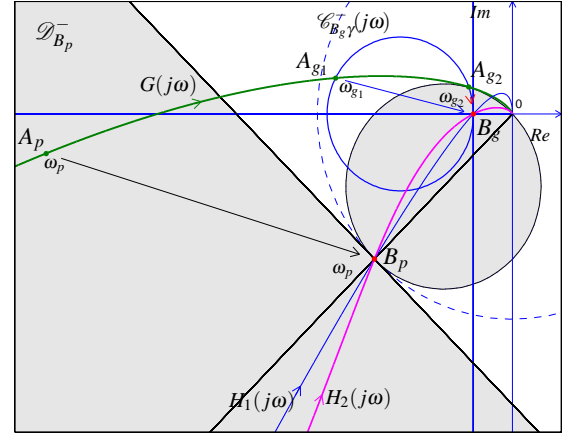


Fig. 9. Graphical solution of Design Problem B on the Nyquist plane.

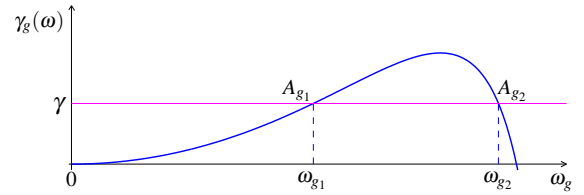


Fig. 10. Plot of function $\gamma_g(\omega)$ versus ω_g .

$-1/G_m$ and $\gamma = \frac{X_p}{Y_p}$, see Fig. 9. If there are no intersections between $\mathcal{C}_{B_g\gamma}^-(j\omega)$ and $G(j\omega)$ the Design Problem has no solutions. Otherwise let $A_{gi} = \{A_{g1}, A_{g2}, \dots\}$ denote the set of intersections points of circle $\mathcal{C}_{B_g\gamma}^-(j\omega)$ with $G(j\omega)$ at frequencies $\omega_{gi} = \{\omega_{g1}, \omega_{g2}, \dots\}$. These points can also be obtained numerically solving the following relation

$$\gamma = \gamma_g(\omega_g) = \frac{\frac{M_{B_g}}{M_{A_g}(\omega_g)} - \cos(\phi_{B_g} - \phi_{A_g}(\omega_g))}{\cos(\phi_{B_g} - \phi_{A_g}(\omega_g)) - \frac{M_{A_g}(\omega_g)}{M_{B_g}}}, \quad (13)$$

or graphically as shown in Fig. 10.

Step 4. For each $\omega_g = \omega_{gi}$, calculate δ and ω_n as follows

$$\delta = Y_p \frac{\omega_n^2 - \omega_p^2}{2\omega_n \omega_p}, \quad (14)$$

$$\omega_n = \sqrt{\frac{X_g \omega_g - X_p \omega_p}{\frac{X_g}{\omega_g} - \frac{X_p}{\omega_p}}} = \sqrt{\frac{Y_g \omega_g - Y_p \omega_p}{\frac{Y_g}{\omega_g} - \frac{Y_p}{\omega_p}}}, \quad (15)$$

where $X_g = X(A_g, B_g)$ and $Y_g = Y(A_g, B_g)$ are obtained using (6) and $A_g = G(j\omega_g)$. The solutions are acceptable only if δ and ω_n are real and positive.

C. Constraint on the complementary modulus margin M_c using loop slope adjustment

The complementary modulus margin M_c is equal to the inverse of the infinity-norm of the complementary sensitivity function $T(s)$, see [11]:

$$M_c = \|T(s)\|_\infty^{-1}, \quad \text{where} \quad T(s) = \frac{G(s)C(s)}{1 + G(s)C(s)}.$$

The margin M_c can be graphically determined as the inverse of the modulus M of the constant M -circle tangent to the open loop frequency response $H(j\omega) = G(j\omega)C(j\omega)$. The margin M_c is an important performance indicator because it is related to the resonance peak of the closed-loop system: M_c is equal to the inverse of the resonance peak for a first-order type system and is equal to the static gain $H(0)$ over the resonance peak for a zero-order type system. Let us consider the following Design Problem proposed in [10].

Design Problem C: (ϕ_m, ω_p, M_c) . Given the control scheme of Fig. 1, the transfer function $G(s)$ and design specifications on phase margin ϕ_m and gain crossover frequency ω_p , design a lead-lag compensator $C(s)$ such that the loop gain frequency response $H(j\omega) = C(j\omega)G(j\omega)$ is tangent in point $B_p = e^{j(\pi+\phi_m)}$ at frequency $\omega = \omega_p$ to the constant M -circle passing on point B_p .

Solution C: *Step 1.* Draw the controllable domain $\mathcal{D}_{B_p}^-$ of point $B_p = e^{j(\pi+\phi_m)}$ as shown in Fig. 11 and check whether the point $A_p = G(j\omega_p)$ belongs to $\mathcal{D}_{B_p}^-$. If not the Design Problem has no acceptable solutions.

Step 2. Determine the parameters $X_p = X(A_p, B_p)$, $Y_p = Y(A_p, B_p)$ using the inversion formulas (6).

Step 3. Calculate the complementary modulus margin M_c related to the unique constant M -circle passing in B_p using the relation

$$M_c = \sqrt{2\cos(\pi + \phi_m) + 2}, \quad (16)$$

and calculate the desired angle ψ of the loop gain frequency response $C(j\omega)G(j\omega)$ in B_p , see Fig. 11, using relation

$$\psi = \left| \arctan \left(-\frac{\cos \phi_m + c_c}{\sin \phi_m} \right) \right|, \quad (17)$$

where $c_c = -\frac{1}{1-M_c^2}$ is the x position of the center of the constant M -circle.

Step 4. Chosen a point $A'_p = G(j\omega'_p)$, where $\omega'_p = \omega_p + \Delta\omega$ and $\Delta\omega$ small, calculate δ and ω_n as follows

$$\delta = Y_p \frac{\omega_n^2 - \omega_p^2}{2\omega_n\omega_p}, \quad \omega_n = \sqrt{\frac{-b \pm \sqrt{b^2 - 4ac}}{2a}}, \quad (18)$$

where

$$\begin{aligned} a &= \alpha_1 + \alpha_2 - \alpha_3, \\ b &= \omega_p^2(\alpha_3 - 2\alpha_2) + \omega_p'^2(\alpha_3 - 2\alpha_1), \\ c &= \alpha_1\omega_p'^4 + \omega_p'^2(\alpha_2\omega_p^2 - \alpha_3\omega_p'^2), \\ \alpha_1 &= Y_D + \tan \psi'(1 - X_D), \\ \alpha_2 &= Y_p \frac{\omega_p'^2}{\omega_p^2} (Y_D Y_p + \tan \psi' (X_p - X_D Y_p)), \\ \alpha_3 &= (X_p - Y_p) \frac{\omega_p'}{\omega_p}, \\ X_D &= \operatorname{Re} \left(\frac{B_p}{A'_p} \right), \quad Y_D = \operatorname{Im} \left(\frac{B_p}{A'_p} \right), \quad \psi' = \psi - \angle A'_p. \end{aligned}$$

The solution is acceptable only if δ and ω_n are real and positive.

Proof: The design specifications define the position of points $B_p = e^{j(\pi+\phi_m)}$ and $A_p = G(j\omega_p)$. According to Prop. 1, the compensators $C_p(s, \omega_n)$ which move point $A_p \in \mathcal{D}_{B_p}^-$ to point B_p are obtained using the parameters γ and δ given

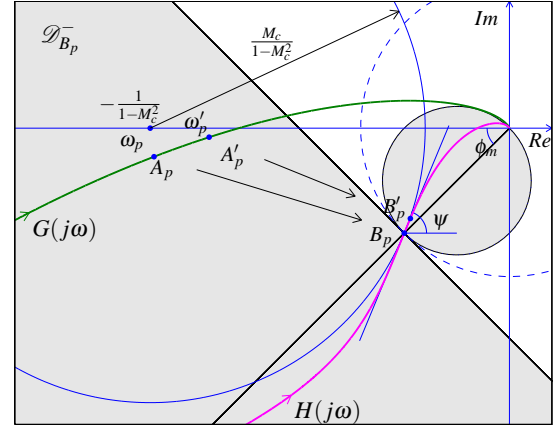


Fig. 11. Solution of Design Problem C.

in (7). The free parameter ω_n can now be used to force the loop gain frequency response $H(j\omega, \omega_n) = C_p(j\omega, \omega_n)G(j\omega)$ to pass through point B_p with slope related to the angle ψ given in (17), see [10]. This problem can be solved using the following condition

$$\lim_{\Delta\omega \rightarrow 0} \angle (H(j(\omega_p + \Delta\omega), \omega_n) - B_p) = \psi. \quad (19)$$

Relation (19) can be approximated choosing a point $A'_p(\omega'_p) = G(j\omega'_p)$ on $G(j\omega)$ at frequency $\omega'_p = \omega_p + \Delta\omega$, with $\Delta\omega$ small, and moving it to point $B'_p = H(j(\omega'_p, \omega_n) = A'_p(\omega'_p)C_p(j\omega'_p, \omega_n)$. From (19) one obtains that

$$\begin{aligned} \angle (B'_p - B_p) &= \angle (A'_p(\omega'_p)C_p(j\omega'_p, \omega_n) - B_p) \\ &= \angle \left(A'_p(\omega'_p) \left(C_p(j\omega'_p, \omega_n) - \frac{B_p}{A'_p} \right) \right) \\ &= \angle (A'_p(\omega'_p) (X_C(\omega_n) + jY_C(\omega_n) - X_D - jY_D)) = \psi. \end{aligned} \quad (20)$$

where $X_C(\omega_n)$ and $Y_C(\omega_n)$ are the real and the imaginary part of $C_p(j\omega'_p, \omega_n)$, X_D and Y_D are the real and the imaginary part of $\frac{B_p}{A'_p}$. Equation (20) can be rewritten as follows

$$\frac{Y_C(\omega_n) - Y_D}{X_C(\omega_n) - X_D} = \tan \psi', \quad (21)$$

where $\psi' = \psi - \angle A'_p$. Equation (21) is a second order equation in the variable ω_n^2 . The solution of this equation provides the value of ω_n given in (18). \square

IV. NUMERICAL EXAMPLES

Consider the unity feedback control scheme in Figure 1, where $G(s)$ has the following structure

$$G(s) = \frac{200}{s(s+1)(s+10)}. \quad (22)$$

Design the compensators $C_p(j\omega, \omega_n)$ that meet the design specification of a phase margin $\phi_m = 45^\circ$ at gain crossover frequency $\omega_p = 2.75$.

1. Calculate ω_n which minimizes the settling time t_s of the step response of the controlled system as described in Design

Problem A.

2. Calculate ω_n to meet the gain margin $G_m = 5$ as described in Design Problem B.
3. Calculate ω_n to adjust the loop slope of $H(j\omega) = C(j\omega)G(j\omega)$ as described in Design Problem C.

Solution. The given design specifications define the points $B = e^{j225^\circ}$ and $A = G(j\omega_p) = 2.4e^{-j175^\circ} \in \mathcal{D}_B^-$, see Fig. 5. The set of compensators (8) that move the point A in B can be obtained using (6) and (7) with $X(A, B) = -0.531$ and $Y(A, B) = -2.52$. The Nyquist plot of $C(j\omega, \omega_n)G(j\omega)$ and the Nyquist and Bode plots of $C(j\omega, \omega_n)$ for $\omega_n \in \{0.3, 0.6, 0.9, 1.35\}$ are shown respectively in Fig. 5-7.

1. Function $\bar{G}(s)$ in (12) is the following

$$\bar{G}(s) = \frac{-0.9174s^4 - 9.091s^3 + 1.826s^2 - 28.64s + 200}{s^5 + 17.94s^4 + 86.31s^3 + 269.4s^2 + 292.2s}.$$

The corresponding root contour is shown in Fig. 8, where the highlighted points correspond to $\omega_n = 0.1 : 0.1 : 1$. The minimum settling time $t_s = 1.72s$ is given for $\omega_n = 0.3$.

2. The parameter $\gamma = \frac{X(A, B)}{Y(A, B)} = 0.21$ and point $B_g = \frac{1}{M_a} = 0.2e^{j180^\circ}$ define the circle $\mathcal{C}_{B_g\gamma}^-(j\omega)$ (see blue circle in Fig. 9). Its intersections points with $G(j\omega)$ are A_{g1} and A_{g2} at frequencies $\omega_{g1} = 4.4$ and $\omega_{g2} = 7.76$. These points can be also obtained solving relation (13), see Fig. 10.

The solution for $\omega_g = \omega_{g1}$ is not acceptable because $\delta < 0$, the corresponding loop gain frequency response is plotted in blue in Fig. 9. The second solution is obtained for $\omega_g = \omega_{g2}$, $\delta = 6.1316 > 0$ and $\omega_n = 0.5436 > 0$, the corresponding loop gain frequency response is plotted in magenta in Fig. 9.

3. Using (16) and (17), the complementary modulus margin is $M_c = 0.7654$ and from (17) $\psi = 67.5^\circ$. Choosing $\omega_p' = 3$, from (18) one obtains $\delta = 3.3748$ and $\omega_n = 0.9143$, the corresponding loop gain frequency response is plotted in magenta in Fig. 11.

V. COMPARISON OF THE METHODS

Usually the synthesis of the three parameters of a second order compensator, such as PID and lead-lag regulator, is done simultaneously on the base of the design specifications. Using Prop. 1 the frequency specifications on the phase margin and the gain crossover frequency can be easily and exactly satisfied. The set of all the closed-loop characteristic equations (11) are linear in the parameter ω_n^2 . This property allows to use the classical root-locus method to find the optimal position of the poles of the closed-loop system to meet the settling time specification. The main disadvantages of this method are that it can not be applied to plants with delays and it requires good knowledge on linear control theory. The second proposed method tries to impose a gain margin specification that, along with phase margin specification, gives a good indicator of system robustness [12]. One of the main advantages of the graphical solution, compared with other graphical approaches such as the one in [13], is that it can be easily determined by ruler and compass in the complex plane by finding the intersections of the frequency response of the plant with particular design circles. Moreover, the proposed

method provides *all* the solutions of the control problem and not only a subset of all the solutions, as it happens in [13]. The main disadvantage of this method is that not always an acceptable solution exists. In the third proposed method the tangency condition of $H(j\omega)$ to the constant M -circle passing through point B_p at the loop crossover frequency guarantees good performance of almost all the closed-loop real systems. In the case of complex high-order systems, however, this specification not always is sufficient to avoid that the loop gain frequency response enters into the constant M -circle at higher frequency. If the method has no admissible solution, it can be extended choosing the value of ω_n that satisfies the equation $\frac{d(\angle(B_p'(\omega_n) - B_p) - \psi)}{d\omega_n} = 0$. Moreover this method is simple because it requires the knowledge of the plant in only two points.

VI. CONCLUSIONS

In this paper the lead-lag compensators have been designed to exactly satisfy the phase margin and the gain crossover frequency specifications. The design has been done using simple inversion formulae. The properties of the obtained compensators are function of a free parameter ω_n . Three different procedures to meet an additional design specification have been presented. Numerical examples show the effectiveness of the proposed methods.

REFERENCES

- [1] W.C. Messner, M.D. Bedillion, L. Xia and D.C. Karns, "Lead and Lag Compensators with Complex Poles and Zeros: design formulas for modeling and loop shaping", *IEEE Control Systems Magazine*, vol. 27, no. 1, pp.44-54, Feb 2007.
- [2] S.S. Flores, A.M. Valle and B.A. Castillejos, "Geometric Design of Lead/Lag Compensators Meeting a Hinf Specification", *4rd IEEE International Conference On Electrical and Electronics Engineering*, Mexico City, Mexico, September 5-7, 2007.
- [3] W. Messner, "Formulas for Asymmetric Lead and Lag Compensators", *ACC American Control Conference*, St. Louis, MO, USA, June 10-12, 2009.
- [4] R. Zanasi, R.Morselli, "Discrete Inversion Formulas for the Design of Lead and Lag Discrete Compensators", *ECC*, 23-26 August 2009, Budapest, Hungary.
- [5] Chen, Y., "Replacing a PID controller by a lag-lead compensator for a robot-a frequency-response approach", *IEEE Transactions on Robotics and Automation*, vol.5, no.2, pp.174-182, Apr 1989.
- [6] K.J. Astrom and T. Hagglund, "Automatic Tuning of PID Controllers", *ISA Press*, 1988.
- [7] G. Marro and R. Zanasi, "New Formulae and Graphics for Compensator Design", *IEEE International Conference On Control Applications*, Trieste, Italy, September 1-4, 1998.
- [8] R. Zanasi, S. Cuoghi and L. Ntogramatzidis, "Analytical Design of Lead-Lag Compensators on Nyquist and Nichols planes", *IFAC World Congress*, Milano, Italy, August 2011.
- [9] Charles L. Phillips, "Analytical Bode Design of Controllers", *IEEE Transactions on Education*, E-28, no. 1, pp. 43-44, 1985.
- [10] D.Garcia, A.Karimi, R.Longchamp and S.Dormido, "PID Controller Design with Constraints on Sensitivity Functions Using Loop Slope Adjustment", *American Control Conference Minneapolis, Minnesota, USA*, June 14-16, 2006.
- [11] D.Garcia, A.Karimi, R. Longchamp, "PID controller design with specifications on the infinity-norm of sensitivity functions", *16th IFAC World Congress*, July, 2005.
- [12] Lee Ching-Hung, "A survey of PID controller design based on gain and phase margins", *International Journal of Computational Cognition*: 2(3):63-100, 2004.
- [13] K.S. Yeung, K.W. Wong and K.L. Chen, "A Non Trial-and-Error Method for Lag-Lead Compensator Design", *IEEE Transactions on Education*, E-41, no. 1, Feb. 1998.